NEW GENERATION OF ULTRASONIC ISPECTION SYSTEM FOR TRAIN WHEELS INCORPORATING BRAKE DISCS

J. L. García[1], E. García[1]
[1] Interlab Ingeniería Electrónica y de Control S.A.

Abstract: This paper deals with the design and operational results of an ultrasonic inspection system specifically designed to detect, in a reliable and repetitive way, the cracks that may develop in train wheels around the brake disk mounting drills.
The system, originally conceived by INTERLAB Ingeniería Electrónica, has been certified by RENFE, the Spanish railroad services operator, as the approved standard for train wheel inspection.

Introduction: High safety standards required in the management of railroad lines, demand the inspection of train wheels during normal maintenance operations, in order to detect the presence of cracks that could seriously affect the integrity of the trains, and therefore passenger safety, should these cracks develop into a complete break of the wheel.
During the last four years, INTERLAB Ingeniería Electrónica (IIE) and ALSTOM have been working on a solution to the problem of ultrasonic detection of cracks that tend to develop around the drills used to mount the brake discs on train wheels, with the main target of creating a system in which inspection of the wheels is performed in service (thus minimising train downtime and reducing maintenance costs), while providing reliable, foolproof crack detection that gives an early warning as cracks begin to develop around the brake-mounting drills.
The crack detection method is based on time of flight domain ultrasound signal processing, which is performed by ULTRASEN®, a fully modular advanced multichannel ultrasonic system developed by IIE.
Two different versions of this system have been fully developed and are currently being used by ALSTOM for the regular inspection of commuter train wheels in its maintenance facilities in Barcelona, Spain. The first version is a portable, manually operated system, which can be moved between facilities as required, whereas the second one is a static version, designed to operate in a semiautomatic fashion and reduce inspection time by a factor of four. A third generation, of which six units are currently being built, is similar in conception and operation to the static version, but includes specific processing oriented to enhance the detection of smaller cracks.
Results: Design of the probe assembly has to meet the main requirement of providing full coverage of the area around each of the wheel's mounting drills, while allowing simple and foolproof crack identification mechanism.
Each wheel is specified to an outer diameter ranging from 890 mm (when new, zero wear) to 810 mm (maximum wear), with six brake disk mounting drills of 32 mm, regularly distributed on a 416 mm circumference (see figure 1).
For obvious practical reasons, the wheel must be inspected while mounted on the train, when direct inspection of the area around the drills is precluded by the presence of different brake and suspension components. In fact, the only free area from which the inspection can be performed is the wheel rolling profile. This implies that a single probe system cannot inspect the complete perimeter of the drills, since the part of the drill farther away from the probe is always obscured by the drill itself (see blue radial beam in figure 1).

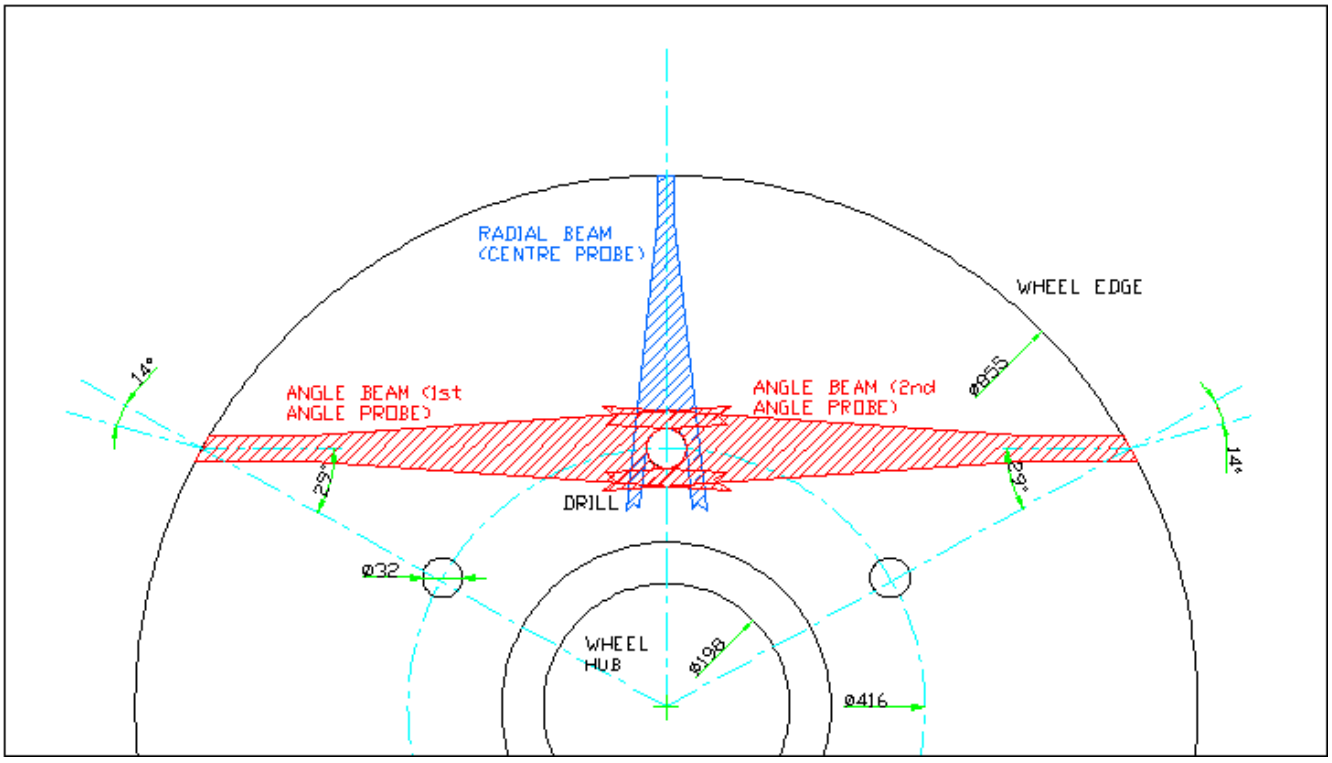

Figure 1. Drill area coverage with single probe vs. three probe inspection

In order to achieve full drill area coverage, the system we present here uses a three probe set-up, so that the central probe axis is aligned with the wheel radius, and the other two are set symmetrically around it, with their axis set at angles of 13º with the wheel radius. For these angled probes, the ultrasound beam refracted into the wheel (transverse waves) is offset around 29º from the wheel radius, so that the three-probe combination allows full coverage of the drill area (see red angle beams in figure 1).

Since the available room around the wheel outer edge is limited, the dimensions of the ultrasound probe set-up must be cut down to a practical size. Thus, the three probes are set as close as possible to each other, so that, when the radial (or centre) probe is inspecting a drill, the angled probes are inspecting the previous and the next one, as shown in figure 2.

The probes are chosen so that each beam covers about twice the diameter of the drill it is inspecting, which calls for slightly larger angular probes, in order to reduce beam spread and thus compensate for the longer distance covered, as shown in figures 1 and 2 (both figures are drawn to scale considering the wheel and probe dimensions). Centre probe diameter is set to 1/2 " (12.5 mm), and angular probe diameter is 3/4 " (19 mm).

Partial immersion coupling is used, with a 5 to 10 mm thickness water layer between the probes and the wheel surface.

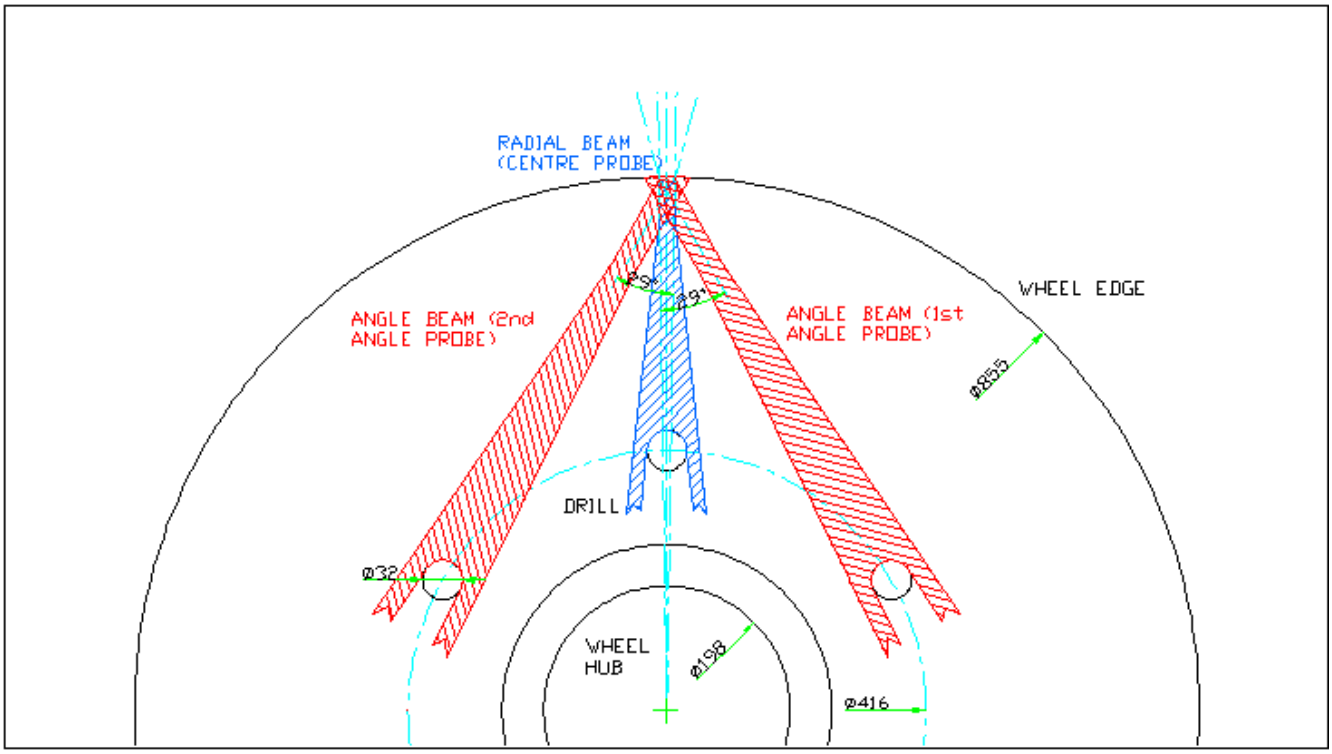

Figure 2. Three-probe set-up for full coverage of the drill area and minimum size

After guaranteeing full coverage of the drill area (see figures 1 and 2 above), we can focus on the main issue in our inspection system, i.e., that of establishing an inspection mode suited to the task of telling damaged drills (those with cracks) from sound ones (those without cracks). To do so, we must analyse how ultrasound pulses coming from the probes are reflected in either case (damaged drills vs. sound drills).

For a sound drill seen from the centre probe (see figure 3), if we consider that the wheel is rotated clockwise while the probe itself remains static, a drill will start producing a significant echo when its upper part enters the probe's ultrasound beam (see position 1 in figure 3). As the wheel rotates, the amplitude of the echo reflected by the drill increases up to the maximum, when the upper part of the drill is perfectly aligned with the probe axis (see position 2 in figure 3). This position also corresponds to the minimum distance between the probe and the drill, or the minimum time of flight for the ultrasonic pulse. From this point on, the behaviour of the reflected echoes is symmetric, with smaller amplitudes and larger times of flight until the wheel rotates to the position where the drill exits the probe's field of view (see position 3 in figure 3).

For sound drills seen from the angled probes (see figure 4), the results regarding amplitude are similar to those expected for the centre probe. The echo amplitude rises as the wheel rotates and the drill becomes aligned with the probe axis (transition from position 1 to position 2 in figure 4), and drops again as the wheel continues rotating and the drill goes out of alignment with the probe axis (positions 2 to 3 in figure 4).

The main difference between the echoes for the angled probes and the central one lies on their time of flight. The time of flight for the angled probes is larger, due to the composite effect of greater drill-probe distance (see fig 3) and lower propagation speed for transverse waves (≈3200 m/s for transverse waves vs. ≈5900 m/s for longitudinal ones). But, most important, is the different behaviour of drill-probe time of flight as the wheel rotates. For the central probe, we already mentioned that time of flight varies only slightly, reaching a minimum value that corresponds to the maximum echo amplitude. On the other hand, for angled probes time of flight shows a wide variation, since drill-probe distance decreases monotonously as the wheel rotates (see positions 1 to 3 in figure 4). In figure 4 we only show angled probe #2 for clarity, but it is apparent from figure 2 that a symmetrical behaviour (with increasing distance or time of flight as the wheel rotates) can be expected for angled probe #1.

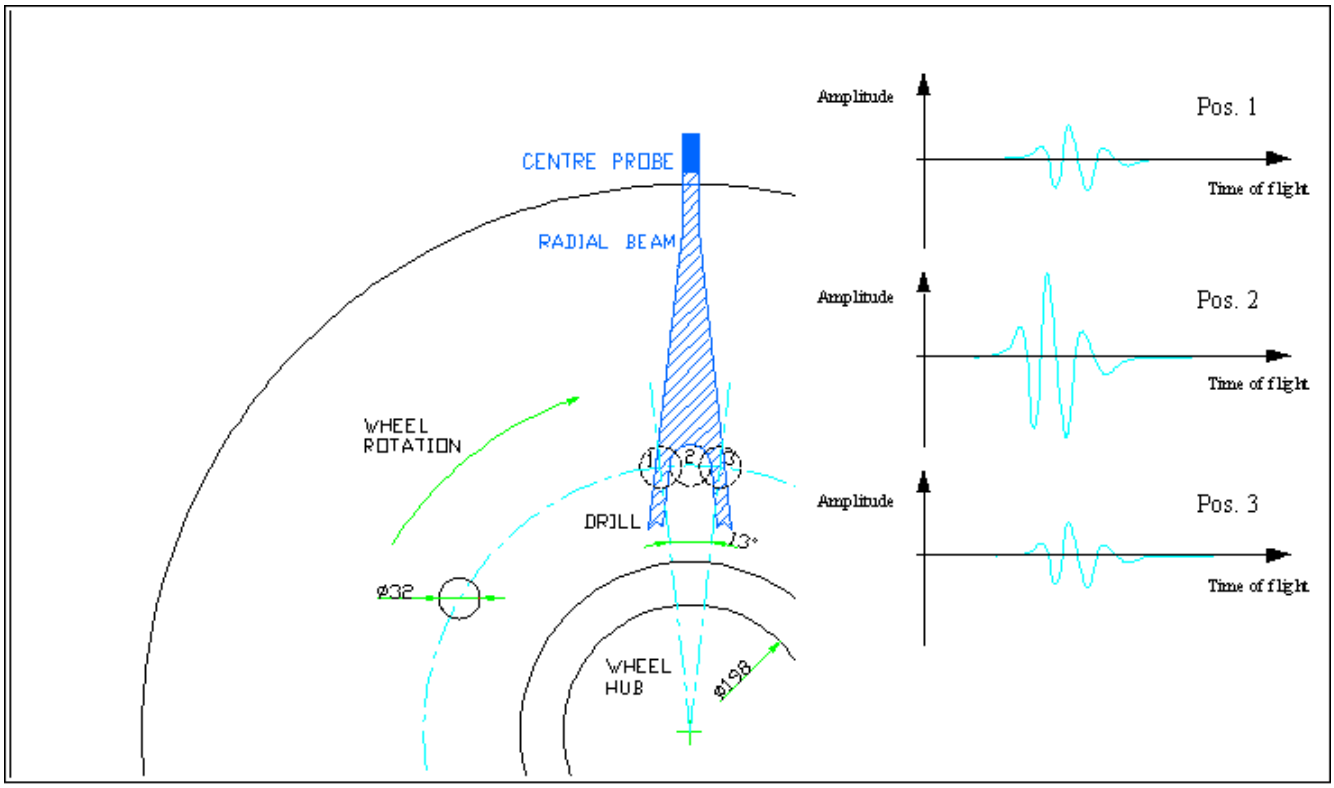

Figure 3. Expected echoes for different positions of sound drill as seen from centre probe

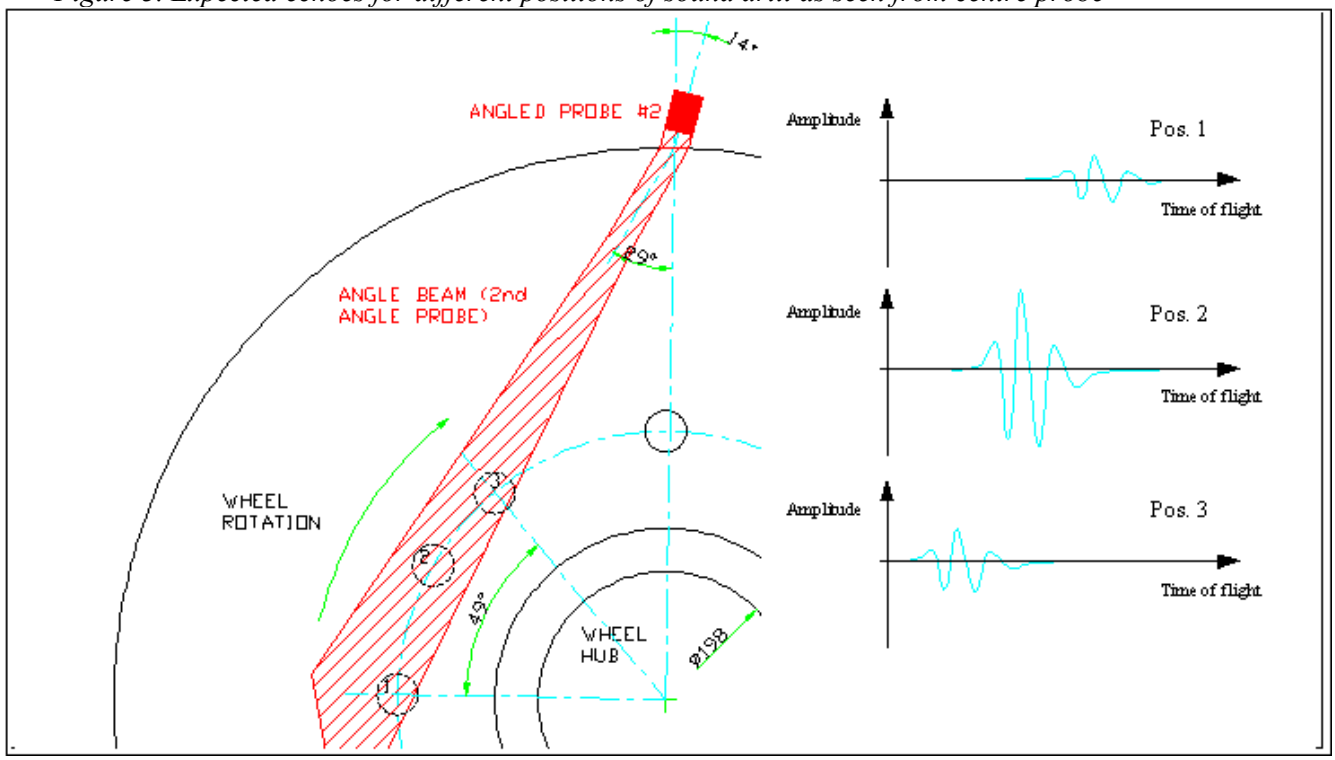

Figure 4. Expected echoes for sound drill as seen from angled probe

As a conclusion, if we plot A-Scans representing the maximum echo amplitude and the corresponding time of flight against the angular position of the wheel for each of the probes, the results should look very similar to those in figure 5. The echo amplitude for each of the probes increases until it reaches a maximum where the drill is aligned with the probe axis, and then drops again until the drill exits the probe field of view.

For the centre probe, time of flight reaches a minimum value when the echo amplitude is maximum, but the overall time of flight variation is relatively small. For the angled probes, time of flight varies widely as the wheel rotates, increasing for probe #1 and decreasing for probe #2.

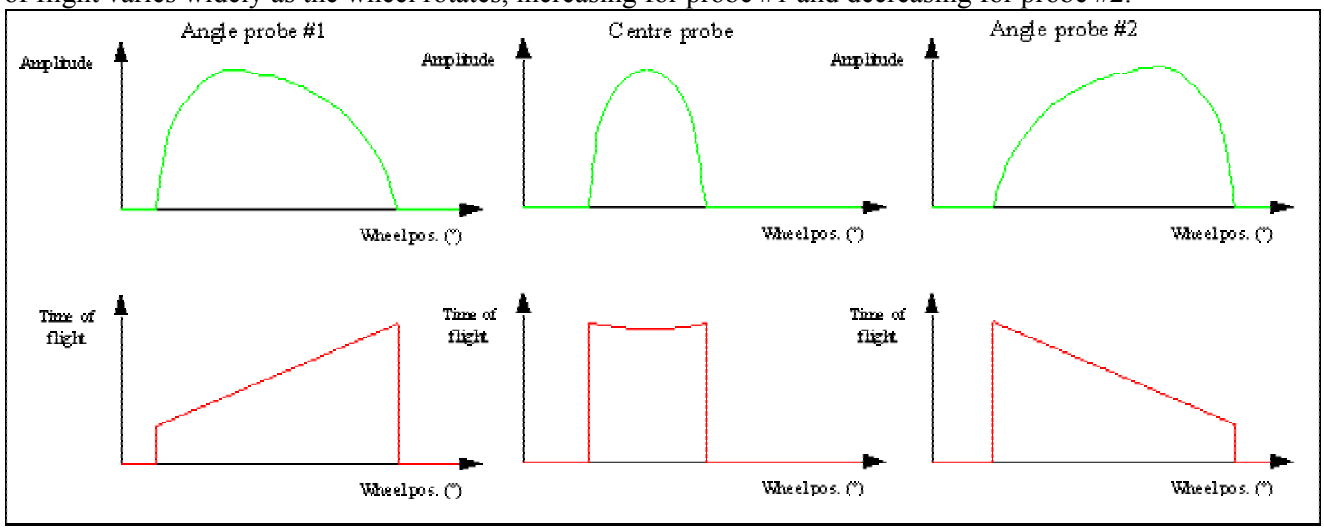

Figure 5. Expected A-Scans for sound drills

The cracks in a damaged drill will be detected by either the centre probe or at least one of the angular ones. Although some of the cracks can be simultaneously detected by two different probes (see results section), here we shall consider only the probe that allows easier detection for each kind of crack.

When the crack direction is more or less orthogonal to the wheel radius, as shown in figure 6, the centre probe starts receiving its echo before it receives the one coming from the drill itself and, as the wheel rotates, the drill echo increases as the crack echo drops, until it is reached a point where the drill echo becomes larger than the crack echo (see figure 6, where a crack is shown on the right side of the drill). The important point is that both echoes are separated in time of flight by the radial distance between the crack and the top of the drill.

When the cracks are more or less aligned with the wheel radius, the situation is similar, but the best-oriented probes to detect them are the angled ones.

Now, we can plot the resulting echoes for damaged drills in A-Scans representing amplitude maximum and time of flight against wheel angular position. The crack shows as a step in the time of flight plot, that should be observed at the point where the amplitude of the crack echo overcomes (or is overcome by) that of the drill, as shown in figure 7.

Thus, cracks around the drill perimeter will show in the time of flight A-Scan, which becomes the basic tool for crack detection in our system. Furthermore, the portion of wheel rotation angle in which the crack echo overcomes the drill echo will depend on the crack size, so that the evolution between inspections of a detected crack can be analysed by comparing the scans. If the crack portion of the A-Scan becomes larger, the crack is increasing in size, whereas if the crack portion of the A-Scan remains constant, the crack is not growing. It must be noticed that this crack size analysis is only relative i.e., you can assert whether a given crack is increasing, but not its absolute size. This is due to the fact that the crack visibility in the A-Scan is affected by factors apart from size, such as angular orientation.

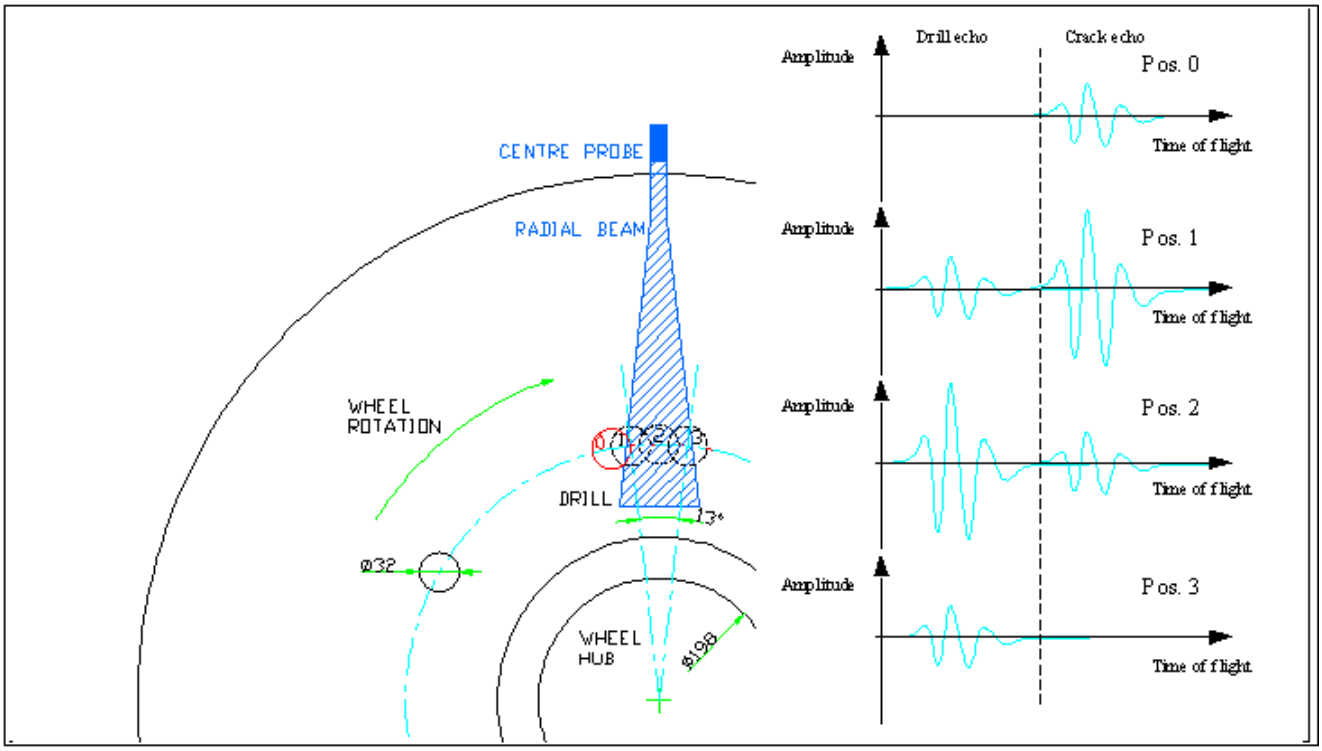

Figure 6. Expected echoes for damaged drill as seen from centre probe

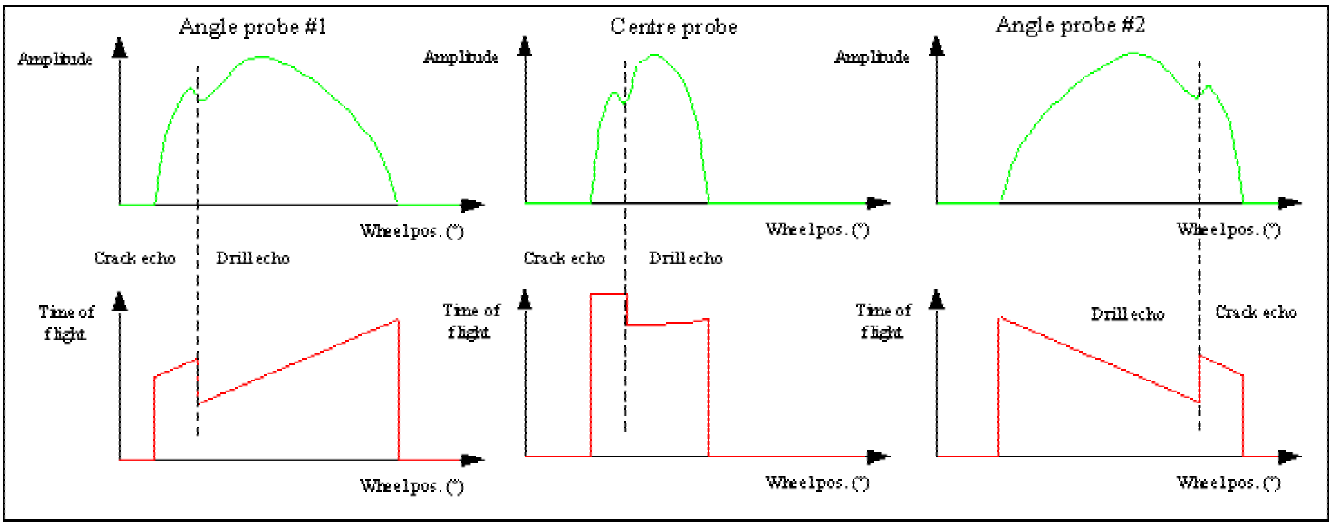

Figure 7. Expected A-Scans for damaged drills with radial (angle probes) or transverse cracks (centre probe)

Discussion: With the inspection method described in the preceding section, a crack is only detected when its reflected echo is larger than the one reflected from the drill itself. This is certainly enough as regards safety concerns, since cracks are always detected before their size represents a hazard to wheel integrity. However, early detection of cracks (when they begin to develop around the drill) can be a powerful tool for predictive maintenance and help reduce overall maintenance cost and train downtime.

In order to achieve detection of smaller cracks time of flight domain signal processing was modified by using two detection windows per probe. The first window is centred around the drill echo using echo-start and pre-trigger on the captured echo signal. A second detection window uses delayed echo-start to cover the area behind the drill echo, where echoes from potential

cracks are expected to appear. In this way, the size of detectable cracks is not limited to those producing an echo larger than the drill, as shown in figure 8.

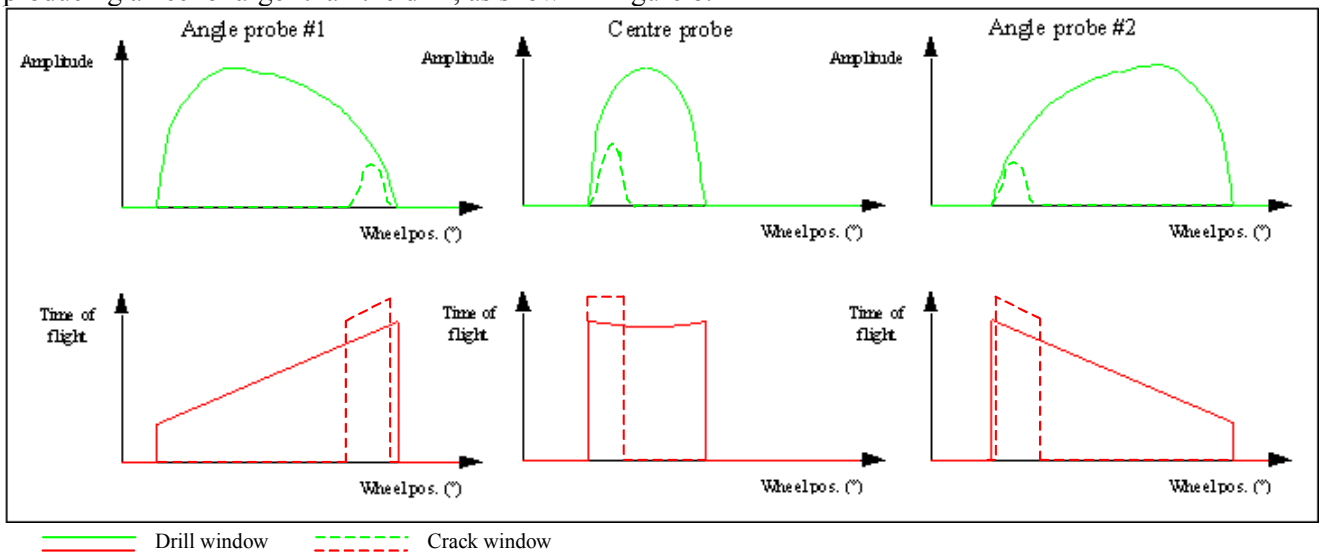

Figure 8 Enhanced detection of small cracks with double window processing

Conclusions: The inspection system described throughout this work, designed to inspect train wheels for cracks developed around the brake-mounting drills, is currently being used by ALSTOM in its maintenance facilities in Barcelona, Spain, for the regular inspection of commuter train wheels, and has been certified by RENFE, the Spanish railroad services operator, as the approved standard for train wheel inspection.

It must be noted that this is not a laboratory method, but a complete industrial inspection system that provides efficient and reliable crack detection covering the complete drill area without taking apart the wheel from the train, something impossible to achieve with a conventional system.

The static, automated version of the system (see figure 12), cuts down wheel inspection time to only 2 hours per train.

Figure 11. Train in position on the inspection system (left) and detail of mounted wheel being inspected (right).